Journal of Natural Products Discovery

https://openjournals.ljmu.ac.uk/JNPD/index

ISSN 2755-1997, 2025, Volume 4, Issue 1 (Article 3240)

Original Article

3D Printing of Multilayered Hydrogel containing Hyaluronic acid and Linalool

Punnatron Kongsithiseth, Satyajit D. Sarker, Touraj Ehtezazi

1. School of Pharmacy and Biomolecular Sciences, Liverpool John Moores University, Byrom Street, Liverpool, L3 3AF, UK
2. Centre for Natural Products Discovery, School of Pharmacy and Biomolecular Sciences, Liverpool John Moores University, James Parsons Building, Byrom Street, Liverpool L3 3AF, UK

D.O.I. 10.24377/jnpd.article3240

Received 18 July 2025; Accepted 28 July 2025; Published 17 September 2025

ABSTRACT

Introduction: This study presents the development of three-dimensional (3D) multilayered printed hydrogel formulations containing hyaluronic acid (HA) and linalool (LN) for potential use as a personalised moisturising and anti-acne product. Various shapes were printed via 3D printing for personalised applications. However, characterisation was mainly conducted on the first layer of the printed hydrogel as representative of the overall structure.

Aims: To formulate, develop, and optimise 3D multilayered printed hydrogel formulations for personalised cosmetic applications, focusing on hydration and anti-acne efficacy.

Methods: Hydrogel formulations containing HA, without LN and with LN (5% and 10% w/w), were prepared by heating and stirring until homogeneous. 3D printing was performed using a thermoplastic printhead (TPP) at 50°C to produce the film. Weight loss under various storage conditions was evaluated. Rheological and mechanical properties were assessed through rheometry and texture analysis, while chemical composition was determined by FT-IR. The release profile of linalool was monitored using HPLC, and antibacterial activity was assessed against *Staphylococcus aureus*.

Results: The average film weight was 2.11 ± 0.20 g, with optimal storage conditions identified as placing the film on a covered plate at 25°C. Films containing 10% LN demonstrated a higher LN release profile (maximum 0.0113 g of the amounts released per g of formulation) compared to the 5% LN films, correlating with stronger antibacterial activity against *Staphylococcus aureus*. FT-IR analysis revealed the absence of C=C and C–H peaks in blank and 5% LN films due to water interference, while 10% LN films displayed characteristic LN peaks. Texture analysis showed that the 5% LN film exhibited greater tensile resistance, with the highest force recorded at 27.500 g. LN played a crucial role in transforming the hydrogel ink into a liquid-like state under high strain.

Conclusion: These findings highlight the potential of 3D-printed HA–LN hydrogels for customisable skincare applications with dual functionality through the inclusion of moisturising components and their antimicrobial effects.

KEYWORDS: 3D PRINTING; HYDROGEL, PERSONALISED SKINCARE; LINALOOL;

INTRODUCTION

The three-dimensional (3D) printing technique is widely known as an additive manufacturing technique that prints the structure layer by layer until it forms a desired structure. This technique is a powerful tool in the fabrication of hydrogel in the shape, size, and structure (Chen et al., 2019). This allows customisation of different designs for hydrogel patches that can be used on different skin areas and treatment needs. Moreover, 3D printing multilayered hydrogels is an innovative type of hydrogel to add some desired personalisation and can be developed to add more active ingredients in the future.

In recent years, hydrogel has gained significant attention in the biomedical and cosmetics industries due to its high water content and ability to mimic tissue for wound healing or personal use (Li et al., 2023, Boriwanwattanarak et al., 2008). In the cosmetics market, many forms of hydrogel have been established, such as gels, creams, and sheet masks, which are usually used for a moisturising effect on facial skin. There are many studies on hydrogel patches used as acne treatments with hydrating ability (Phumlek et al., 2022, Lee et al., 2003). However, there is still a limited number of hydrogel-based formulations that offer both acne treatment and skin hydration using pure linalool and hyaluronic acid, especially in the form of 3D-printed small hydrogel patches (Chelu, 2024, Shin et al., 2019).

Numerous studies have utilised 3D printing technology to develop hydrogel patches for cosmetic applications. For example, 3D printing of hydrogel patches for hydrating and reducing sebum levels using sodium hyaluronate, glycerol, and Camellia sinensis leaf distillate (Manousi et al., 2024). Moreover, the cryptotanshinone-loaded niosomal hydrogel was formulated and characterised for its anti-acne and transdermal properties, with hydrating (Wang et al., 2020). These studies highlight the potential of hydrogel patches produced via 3D printing for cosmetic use. However, this study focuses on the incorporation of linalool and hyaluronic acid as active ingredients for combined anti-acne and hydrating effects.

Hyaluronic acid (HA) is a well-known active ingredient in the cosmetic industry, valued for its hydrating, anti-inflammatory, and anti-irritating properties (Lubart et al., 2019). From previous studies, a high amount of HA is found in young human skin, but it decreases with age (Lubart et al., 2019). The reduction of HA affects skin hydration, which causes skin ageing. Therefore, applying HA on the skin will prevent skin ageing through the moisturising effect. Although HA has a large molecular size that limits permeation through skin, it effectively hydrates the upper epidermis and prevents transepidermal water loss (Bravo et al., 2022).

Linalool (LN) is a monoterpene alcohol found in many plant species with a colourless, strong scent and is highly used in the cosmetics industry (Ehtezazi, 2023). The chemical structure of LN is (CH3)2C=CH(CH2)2C(CH3)(OH)CH=CH2. Linalool can be anti-inflammatory, antimicrobial, and anticancer, but is usually used for antimicrobial activity (Pereira et al., 2018). Linalool can disrupt the bacterial cell wall and inhibit bacterial enzyme activity to prevent the growth of bacteria, especially on *S. aureus, E. coli, and C. albicans* (Pereira et al., 2018).

Based on a previous study, a combination of 1.5% kappa carrageenan (KC) and 1.3% xanthan gum (XG) is an appropriate formulation for 3D printing using BIOX Cellink with a controlled temperature print head (Avallone et al., 2023). In addition, other studies have demonstrated that combinations of sodium alginate (SA) and XG support good printability (Unalan et al., 2023). Inspired by these findings, the present study developed several formulations with varying concentrations of gelling agents, including KC, XG, and SA, to evaluate printability. Glycerin was added to the formulation to enhance printability, as a higher glycerol content enhances the gel's self-support during printing (Li et al., 2024), and to improve skin hydration due to its humectant properties.

This study evaluated square-shaped hydrogels as the base for multilayered patches, focusing on formulations containing both LN at 5% and 10% w/w and HA. A method was developed to determine the LN release profile using a high performance liquid chromatography (HPLC) method over 6 hours. Anti-acne activity was examined through antibacterial testing against *Staphylococcus aureus*. Film stability was assessed via weight loss under different storage conditions. The composition in the film was analysed using Fourier transform infrared spectroscopy (FT-IR), while its physical properties were characterised through texture analysis and rheology.

MATERIALS AND METHODS

MATERIALS

Kappa carrageenan (Special Ingredients, UK), Xanthan gum (Mr.P Ingredients, UK), Sodium Alginate (Sigma-Aldrich, UK), Hyaluronic acid mask powder (Guangdong Tongyan Biotechnology, China, purchased via Amazon), Vegetable Glycerin (The Soapery, UK), Linalool (Sigma-Aldrich, UK), red colouring agent (Tesco, UK) and orange powder (food grade) were used as received.

Methods

Hydrogel formulation

The hydrogel composition and percentage of each formulation are shown in Table 1. Phase A, containing sodium alginate (SA), kappa carrageenan (KC), xanthan gum (XG), glycerin (GR), and deionised (DI) water. Hyaluronic acid (HA) and water are in Phase B, and Phase C contains LN.

Preparation of Hydrogel Films

From Table 1, formulations 5, 6 and 6.1 are the successful printing formulations using this 3D printing technique. The ingredients were weighed into a weighing boat using an analytical balance. GR and DI water were heated on a hot plate at 80-100°C while mixing at 400 rpm by the overhead stirrer. XG and HA were sieved separately using a 100-micron microscopic sieve and weighed to the right amount after sieving. After that, KC (1.5 g) and XG (1.3 g) were gently added to the solution and stirred at 400-600 rpm until a homogeneous mixture was achieved. Meanwhile, HA (0.5 g) was dissolved in DI water by magnetic stirrer for 1 hour, then added to phase A and stirred continuously until a homogeneous mixture was formed. Lastly, for formulations 6 and 6.1, LN was added to the solution and stirred well. The hydrogel ink was then added to the 3D thermoplastic print head, and the parameters and shape were adjusted for printing. Other formulations were using the same method with different compositions of gelling agent and HA, as shown in Table 1.

Pink hydrogel ink was prepared using 1 drop of red colouring agent in 50 g of hydrogel ink, while the red cross sign was prepared using 10 drops of red colouring agent in 40.4317 g of base hydrogel. The yellow colour was prepared by adding 0.0262 g of orange powder to 37.9185 g of hydrogel base.

3D printing hydrogel film

A BIOX Cellink 3D printer, equipped with a thermoplastic print head, was used to print multilayered hydrogel. The sample was added to the thermoplastic printhead (TPP) with a 0.2 mm diameter nozzle, and the print head was controlled at a temperature of 50°C. Pressure was applied at 6 kPa, and the speed was set at 30 mm/s to print the hydrogel. Hydrogels were printed as rectangles (20.37 x 50.00 x 1.67 mm), squares (30.00 x 30.00 x 1.00 mm), hearts (25.00 x 21.10 x 1.11 mm), stars (22.00 x 21.72 x 1.00 mm) and cross signs (12.00 x 12.00 x 0.50 mm). A multilayered hydrogel film was printed in a square shape and allowed to set before printing the other shapes on top of it. For the third layer, the heart shape was allowed to set, and the cross sign was printed on top. The heart, star, and cross sign were printed at a speed of 25 mm/s.

Weight loss

Hydrogel square 3D printed films of 5% LN were weighed after printing on the plate and then again at 15, 30, 45, and 60 min. The weight loss was compared across three storage conditions: with and without covering the plate at room temperature and covering the plate in the fridge. Three replicates were performed. Weight loss was calculated using equation 1.

$$\text{Weight loss (\%)} = (W_i - W_t)/ W_i \times 100 \quad [1]$$

Where W_t is the weight of samples at time t, and W_i is the initial weight of samples.

Linalool Release Profiles from Hydrogel Films

The square hydrogel films with 5% or 10% LN were weighed using an analytical balance and added to the MEMBRA-CEL MD34 cellulose membrane. The film was then put in the 250 mL beaker, and 100 mL of water was added and then placed on a hot plate set to a temperature of 32°C. The overhead stirrer was set at 97 rpm and stirred above the gel, ensuring not to touch the gel and cellulose membrane. Six samples were collected every hour over 6 hours, and each was taken at 1 mL using a 2.5 mL syringe with a needle, then filtered through a 0.45 µm nylon filter into the HPLC vial. After that, the cap was secured onto the vial. 1 mL of deionised water was added back to the system after taking a sample. After that, the quantification of LN was evaluated using HPLC. Three replicates were performed.

An 11-point calibration curve for LN in water was prepared with solutions in the range of 0-500 µg/mL. LN (50 mg) was weighed and dissolved in 100 mL of DI water to prepare the stock solution at a concentration of 500 µg/mL, then serial dilution was performed from this stock solution using DI water. 11 samples were prepared using 10 mL volumetric flasks, and 1.00 mL was taken to be filtered through a 0.45 µm Nylon filter into an HPLC vial.

High Performance Liquid Chromatography (HPLC)

The HPLC method was done in the same way as the previous study (Ehtezazi, 2023). An Agilent 1200 series HPLC was used to analyse the LN content of the hydrogel film. The LN (97%) was analysed using a reversed-phase C-18 column (4.6 x 150 mm, 5 µm), using acetonitrile and water (35/65 v/v) as a mobile phase with a flow rate of 1.0 mL/min. The column temperature was set to 25°C, and the detection spectrophotometer was set at 210 nm, with an injection volume of 5 µL. Each HPLC run was performed for 5 min, with an additional 2 min post-run.

Antibacterial activity

A total of nine samples of square hydrogel were printed. Three were blanks without LN, three contained 5% LN, and the remaining three contained 10% LN. The sample was then put separately in a plate of agar with 0.2 mL of *Staphylococcus aureus (S. aureus)*. Lastly, 3 plates were control plates, containing only *S. aureus*. A total of 12 plates of samples were left for 2 days and observed for bacterial growth.

Fourier transform infrared spectroscopy (FT-IR)

An Agilent Cary 630 FTIR was used to determine the composition of the hydrogel. Nine hydrogel square samples were printed; three of which were without LN (blank), three contained 5% LN, and the others contained 10% LN. An aqueous LN solution was used as a reference. The sample was placed on the machine plate, and the probe was lowered to touch the surface of the sample to commence the process.

Texture Analyser

A TA.XT Plus was used to analyse the texture of hydrogel films. Three films were printed without LN, three contained 5% LN, and the last three contained 10% LN. The texture analyser machine was calibrated to measure the height and determine the size of each hydrogel film before running, using a Vice action tensile grip as a probe. Test speed and post-test speed were set at 3.00 mm/sec. Target mode was in distance mode, which was set at 10.00 mm.

Rheological analysis

The TA HR10 rheometer was used to analyse the rheology of hydrogel inks with three different compositions. One without LN (blank), one contained 5% LN, and the last one contained 10% LN. The sample was then added to the probe. The test was set with a gap of 200 µm, 50°C, and a 30-second soak time. Three replicates were performed for each batch of samples.

RESULTS

Table 1 presents the development of the hydrogel ink formulation with different compositions, shapes and printing parameters, as well as the appearance after printing of each formulation. Printer head: A Pneumatic and thermoplastic printer head (TPP) was used to print formulations with different nozzle sizes, pressures, and temperatures.

Table 1: Summary of hydrogel formulation and printing parameters.

Formulation	%w/w								Printer head	Nozzles (mm)	Pressure (kPa)	Temperature (°C)	Appearance after printing
	Phase A					**Phase B**		**Phase C**					
	SA	KC	XG	GR	Water	HA	Water	LN					
1	3	-	1.5	-	50	0.5	45	-	Pneumatic	0.410 (22G)	15-24	25	

2	-	2	-	3	54.5	0.5	40	-	Pneumatic	0.410 (22G)	6	50-60	
									TPP	0.410	6	50	
3	-	2	-	3	54	1	40	-	TPP	0.410	6-16	50	
4	-	2	0.5	3	54	1	40	-	TPP	0.410	6-10	50	
5	-	1.5	1.3	3	53.7	0.5	40	-	TPP	0.200	6	50	
6	-	1.5	1.3	3	68.7	0.5	20	5	TPP	0.200	6	50	
6.1	-	1.5	1.3	3	63.7	0.5	20	10	TPP	0.200	6	50	

Figures 1A, 1B and 1C show a photograph of further personalised film with a star, heart, and a heart with a cross shape printed on the base square hydrogel and presented as a multilayered hydrogel film. Figures 1D and 1E present a photograph of multilayered films after leaving for two days.

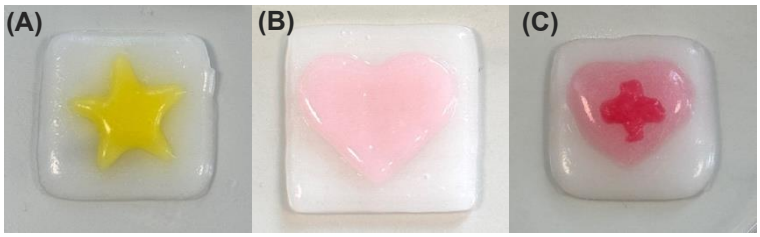

(D) **(E)**

Figure 1: Appearance of the multilayered films: (A) a star and (B) a heart as a second layer, (C) a cross sign as a third layer on a square base, (D) a star, and (E) a heart after two days of storage.

Figure 2 presents the average percentage of water loss from the hydrogel film with different storage types, which are the room temperature with and without lids and in the fridge with lids, observed over 1 hour. The results show that keeping it at room temperature with the lid on results in a weight loss of 2.05% in 1 hour. The weight loss reaches 8.55% when the sample is kept at room temperature without the lid, and 2.80% of water was lost from the film after storing it in the fridge with the lid. The weight differentiation was observed at 2.11 ± 0.20 g.

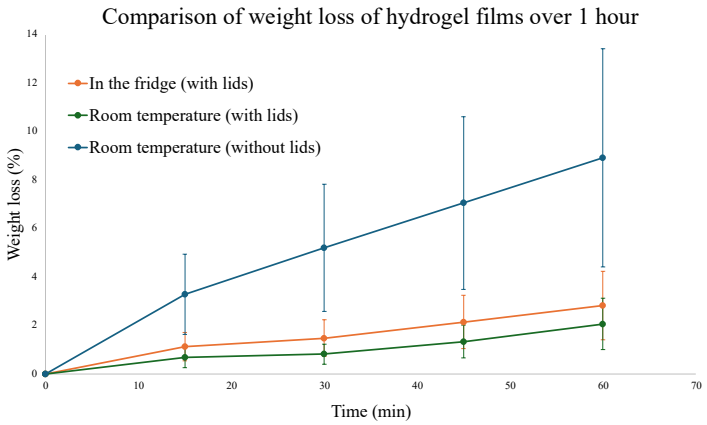

Figure 2: The comparison of weight loss of hydrogels stored at room temperature (without lids), in the fridge (with lids), and at room temperature (with lids). Error bars represent SD (n=3).

Figure 3 presents the calibration curve for the LN solution in water with the concentration from 0 to 500 µg/mL. An excellent linear line was shown with an R^2 of 0.9989.

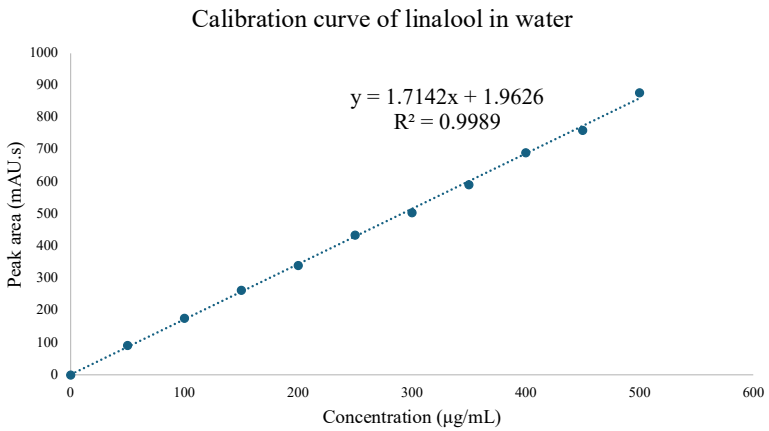

Figure 3: Calibration curve for LN in water from 0 to 500 µg/mL.

Figure 4 represents the comparison of the LN released from 5% and 10% LN in the film. After 6 hours, the 10% LN film showed a greater release, with the amount of 0.0113 g per gram of formulation, compared to 0.0104 g from the 5% LN film.

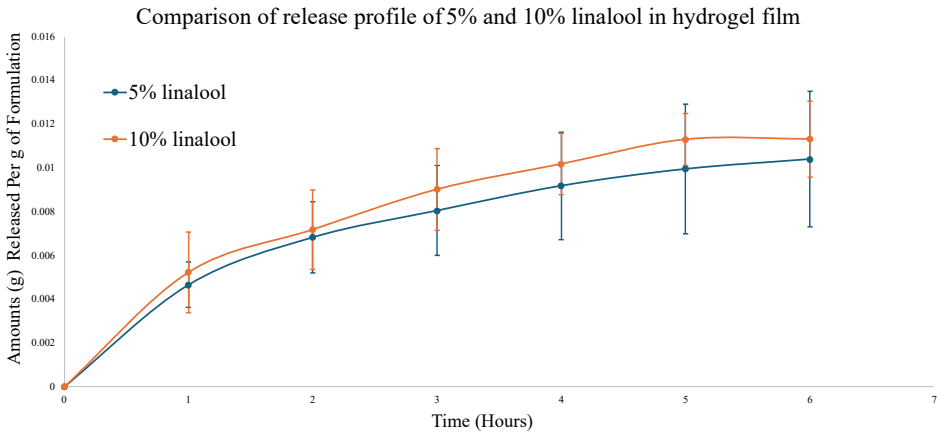

Figure 4: The comparison of the LN release profile between 5% and 10% LN films. Error bars represent SD (n=3).

The antibacterial activity was performed with a control, a blank film, a 5% LN film and a 10% LN film in an environment of *S. aureus*. After 2 days, the results in the photograph are shown in Figure 5. *S. aureus* was observed in all areas on the control and blank film plates, whereas no bacterial growth was detected on the 10% LN film plate. In contrast, limited bacterial growth was found on the 5% LN film plate, primarily at the right and bottom edges of the film, with no growth observed on the left side.

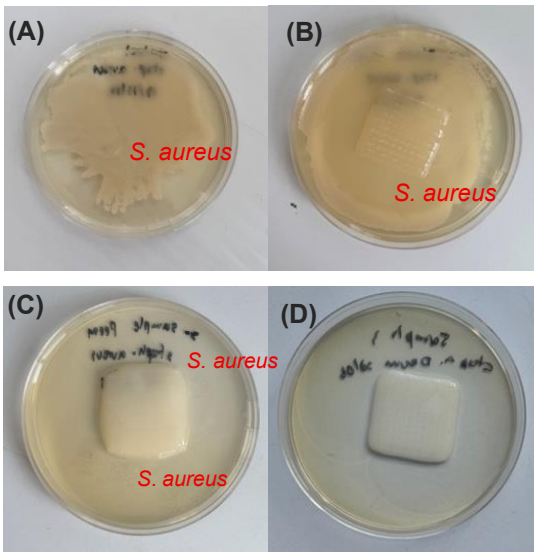

Figure 5: Growth of *Staphylococcus aureus* in (A) a control, (B) blank film, (C) 5% LN film, and (D) 10% LN in hydrogel films.

One replicate of the FT-IR spectra of LN solution, blank film, 5% LN, and 10% LN in hydrogel film are shown in Figure 6. The spectrum of blank and 5% LN is similar, with a large, broad peak between 3000 and 3700 cm^{-1} and a sharp peak at 1650 cm^{-1}. In contrast, the FT-IR spectrum of the 10% LN film showed the same broad and sharp peaks as those of the blank and 5% LN films. However, very sharp peaks appeared around 850-1400 cm^{-1} in 10% LN film, showing a similar characteristic to the LN solution peaks, whereas blank and 5% LN film did not.

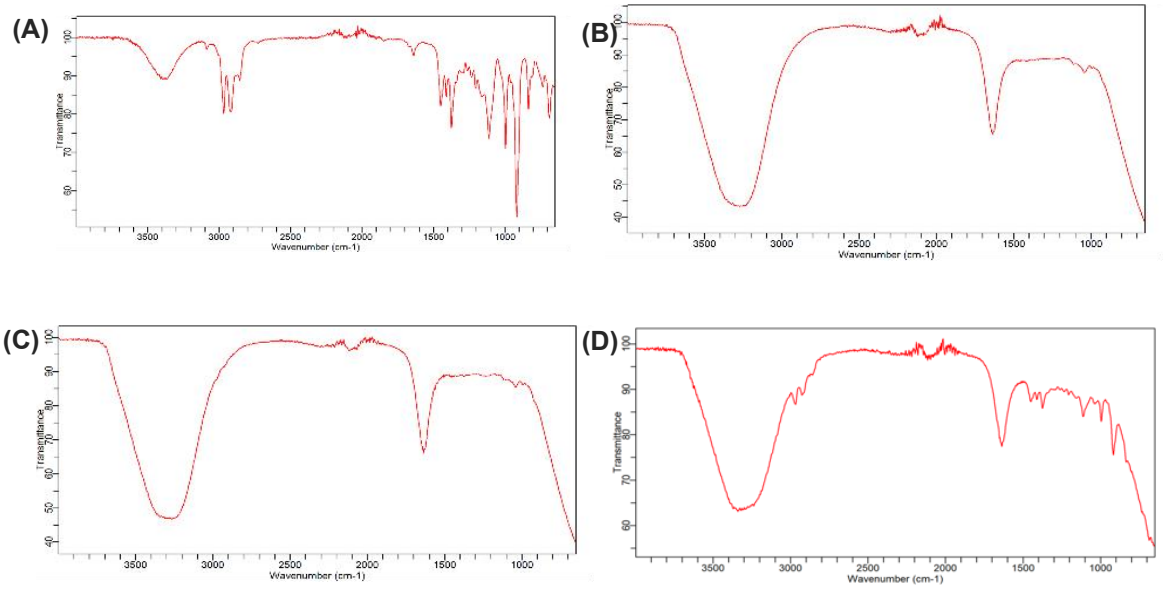

Figure 6: FT-IR spectrum of (A) LN solution, (B) blank, (C) 5% LN in film, and (D) 10% LN in film.

Figure 7 shows the resistance to tear profile analysis (TPA) of blank, 5% LN film, and 10% LN film, with the comparison of average stress (kg/mm^2) and strain (%) from three replicates. The average highest force from three replicates used to break the blank film is 2.035 g with an average stress of 2.175 x 10^{-6} kg/mm^2, while the average highest force used for the 5% LN film is 27.500 g with an average stress of 3.055 x 10^{-5} kg/mm^2. Moreover, the 10% LN film was used at a force of 2.274 g and 2.180 x 10^{-6} kg/mm^2 to break the film.

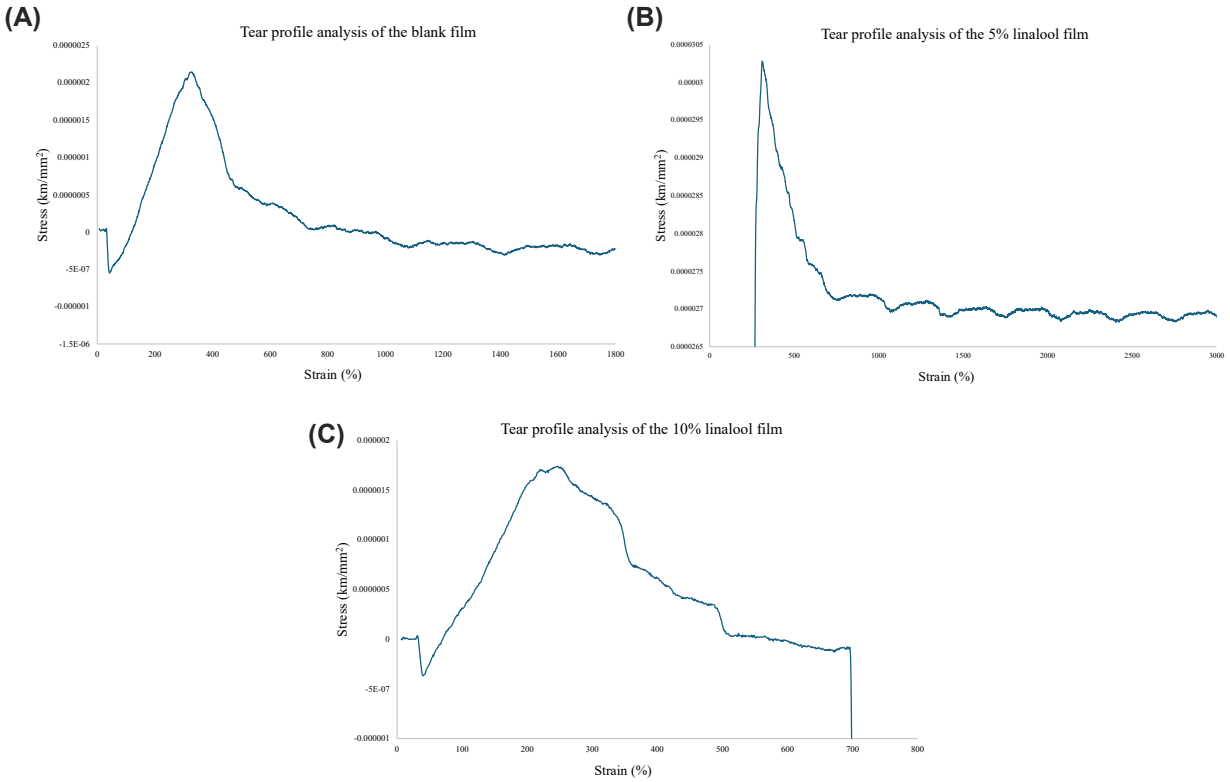

Figure 7: Stress and strain curve of (A) blank, (B) 5% LN, and (C) 10% LN in hydrogel film.

Figure 8 presents the rheogram of blank, 5% LN hydrogel ink, and 10% LN hydrogel ink, with the comparison of average storage modulus G', loss modulus G", complex viscosity η*, and oscillation strain from three replicates. All results show that G', G'', and η* decrease as strain increases. In the blank hydrogel ink, G' is higher than G" from low to high strain, whereas 5% LN and 10% LN hydrogel inks behave differently. The crossing point of G' and G" was observed in the 5% LN hydrogel ink at around 1000% strain, while the 10% LN hydrogel ink exhibits a fluctuating crossing point at approximately 100% strain. However, at a very low strain (<1%), G', G'', and η* remain constant in every sample.

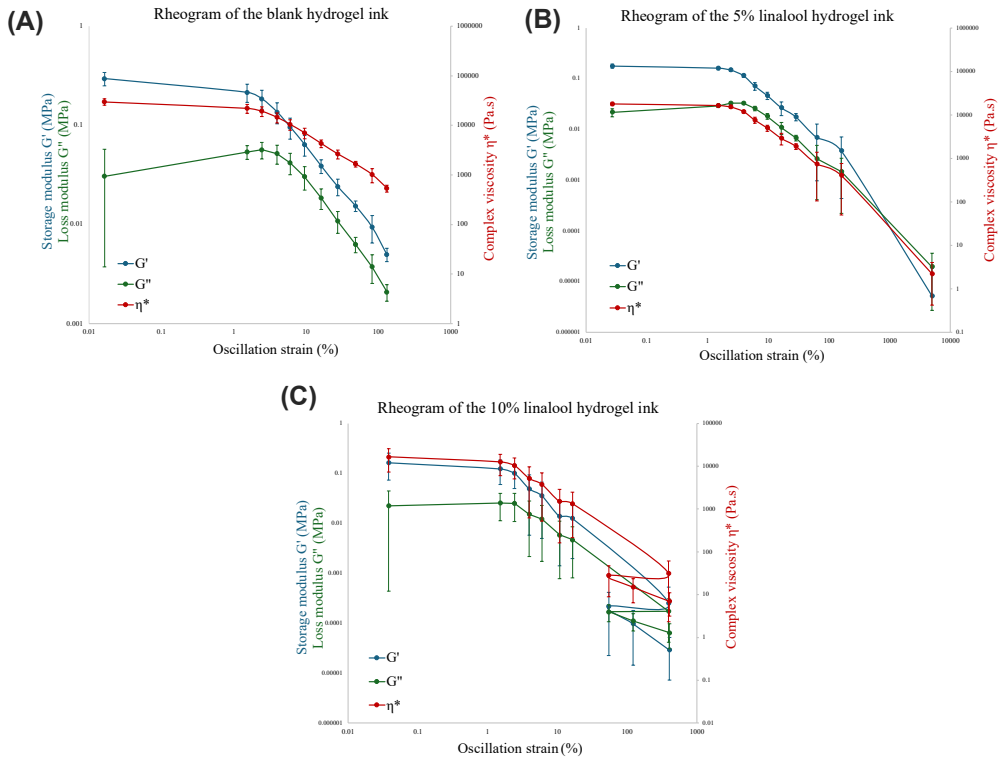

Figure 8: The rheogram of (A) blank, (B) 5% LN, and (C) 10% LN hydrogel ink. Error bars represent SD (n=3)

DISCUSSION

The hydrogel formulations were developed to find an excellent formulation for the 3D printing technique. The first formulation used SA and XG as a base gel, following the previous study (Unalan et al., 2023). After printing, the gel was cross-linked with 0.1 M $CaCl_2$ using a plastic pipette and printer head; the gel was not well-structured, as shown in Table 1. In contrast, these results differ from the previous study using the same formulation due to the different parameters and 3D printer model (Unalan et al., 2023). Then, a formulation was developed to utilise KC and GR; however, the temperature gradient of the pneumatic printer head caused an ink blockage at the tip of the nozzle, resulting in a non-uniform structure. After switching to the TPP printer head, the formulation continuously flowed out of the nozzle tip and caused a blockage. Additionally, 6 kPa pressure was used for printing, but the formulation was extruded excessively without forming a filament line. Then, formulation 3 was developed to observe how HA affects printing ability. However, no significant improvement in printability was observed. The hydrogel remained overly fluid, resulting in downward flow and accumulation at the nozzle tip. Therefore, XG was added to the formulation to expect better printability. However, a massive solution came out due to the liquidity and blockage of white flakes from XG and HA, with the rapid film formation of the formulation still causing a problem of continuous printing. Formulation 5 was developed with sieving XG and HA, and it was successful in printing the square shape, as shown in Table 1. Increasing the amount of XG solves the problem of excessive liquidity and rapid setting of the formulation, while the sieving method causes no blockage at the tip of the printer head. These findings gave the definitive result with a printable hydrogel, like the inspired formulation from the previous study (Avallone et al., 2023). Then, different percentages of LN were added to the formulation. As LN is a volatile compound, it was decided to add it at the last step of mixing to prevent loss and maintain its ability. Even though LN is slightly soluble in water (Gonçalves et al., 2020), it was dispersed easily in the gel. This apparent compatibility is not due to actual dissolution but rather due to several physicochemical mechanisms of XG, KC and GR that help stabilise LN in the system.

The multilayered hydrogel was designed with different shapes for the second and third layers to create a personalised film. Heart and star shapes were precisely printed using formulation 6 on the square base. The third layer was printed as a cross, as shown in Figure 1C. After printing, there is no sign of separation between each layer. The pink and red colours came from a liquid red colouring agent, while the yellow was from orange colour powder. After two days, the yellow dispersed into a square shape, but this did not occur with the red or pink colours, as shown in Figures 1D and 1E. This observation revealed that the colouring agent in powder easily passes through the different layers of gel, whereas the liquid colouring agent does not. This could lead to the idea of using other powdered active ingredients in the second layer to give a different function in the future.

The characterisation was performed using formulation 5 as a blank, 6 with 5% LN, and 6.1 with 10% LN. First, the film's weight loss was analysed to determine the optimal storage method, as shown in Figure 2. The results show that the best storage method is to keep it at room temperature with the lids on, with only a 2.05% weight loss. In contrast, the weight loss reaches 8.55% when the sample is kept at room temperature without lids. However, in theory, keeping samples in the fridge should be the best way to prevent water loss, as evaporation occurs more slowly. This variation in weight may be caused by the film's weight differences, which can affect water loss; specifically, the lighter film loses more water. Although three replicates were performed, weight differentiation was still observed at 2.11 ± 0.20 g, which could be due to minor inconsistencies in sample preparation or structural changes during printing. Temperature variations when removing samples from the fridge every 15 min may also influence the rate of water evaporation. Therefore, these factors can significantly affect weight loss results and may lead to findings that differ from theoretical expectations.

Second, the release profiles were observed. A MEMBRA-CEL MD34 cellulose membrane was used to stimulate the diffusion of substances from the film to the skin while preventing large substances from passing through the membrane (Wang et al., 2024). Therefore, the experiment was set at a temperature of 32°C, as it is the usual human skin temperature. The content of LN was analysed using HPLC and shows an increasing trend in release, as shown in Figure 4. The comparison showed that 10% LN film released a greater amount of LN than 5% LN film over 6 hours, reaching 0.0113 g per gram of formulation. Therefore, an increased amount of LN in the film leads to a higher release-concentration of LN to the skin. Like the 3D printed film of SA and XG containing clove essential oil. The higher amount of oil in the film was released more than the lower one (Unalan et al., 2023).

Third, the antibacterial activity of the film was assessed. *S. aureus* was noted at the edge of one side of the 5% LN hydrogels, though the other side was nearly clear. This is because the linalool may evaporate and cause bacterial growth. In contrast, no microorganism was observed in the 10% LN film, as shown in Figure 5. Control and blank gave the same results, as the growth of bacteria was noticed. Other studies found that basil oil, which contains a high amount of LN had antimicrobial activity against *S. aureus*, *B. subtilis*, *E. coli*, and *Aspergillus niger* (Hussain et al., 2008). Similar to our results that 10% LN has a higher antibacterial activity than the 5% LN film against *S. aureus.*

Next, the FT-IR spectra shown in Figure 6, LN spectra have a very sharp single peak around 850-900 cm^{-1} corresponding to the C=C stretch, which is considered as vinyl and vinylidene in the LN structure. The peak at 1100 cm^{-1} indicates a C-O stretching, while the sharp peak at 1350 cm^{-1} corresponds to a C-H bend, and CH_2 / CH_3 bending shows a peak at 1450 cm^{-1}. A small sharp peak at around 1640 cm^{-1} is attributed to C=C stretching. C-H stretch showed a peak at around 2850-2950 $cm^{-1,}$ and the O-H bond is characterised by a broad peak at around 3400 cm^{-1} (Menezes et al., 2014). Previous study suggests that the most important characteristic of LN is the peak of the C-O group at 1000 cm^{-1} (Menezes et al., 2014). The blank hydrogel and 5% LN film gave the same results with a sharp, strong peak at 1650 $cm^{-1,}$ showing the C=C stretching, and a strong, broad peak at around 3100-3600 cm^{-1}, corresponding to the O-H bond. This spectrum shows the C=C and O-H stretches without exhibiting any stretching of the C-O bonds (1000 cm^{-1}), which is a characteristic of LN. This means that the water content in the film may cause the signal to interfere with the signals of the C-O bond. In contrast, when the LN content is increased to 10%, the peak

of C=C, C-O, C-H, and CH_2 / CH_3 bending is found at the same wavelength as LN solution spectra, with a very sharp peak of C=C and a strong broad peak of O-H. These results show that a film with higher LN content has a prominent LN peak compared to those with lower LN content.

From the TPA in Figure 7, the 5% LN film used the highest force at 27.500 g to break the film. These results suggest that the 5% LN film has the highest tensile strength among the tested groups, showing the greatest resistance to elongation and tearing. However, the force value of 5% LN film is far apart from the others, which may be caused by the storage time of the film in the fridge, enhancing the hardness and dryness of the film. Consistent with previous research, the freeze-dried gelatin/alginate 3D printed gel had higher hardness compared to the gel before freezing, while no difference in the hardness of different formulations after freezing due to the hard and dry texture (Kuo et al., 2021). The storage time could have altered the film's physical structure, causing an overestimation of its tensile performance.

Lastly, the rheogram of the blank hydrogel ink shows that G' is higher than G" during the analysis without a cross line, which indicates more elasticity rather than liquidity, as shown in Figure 8. At the minimum strain, the values of G', G", and viscosity suggest that this ink is resistant to breaking. Then, from 1-100% strain, G' and G" decreased, indicating a reduction in elasticity and easier flow due to the decrease in viscosity. Therefore, this ink acts more viscoelastic and solid-like than liquid-like, which is suitable for printing films that need high structural integrity after printing. At lower strain (<1%), the behaviour of 5% and 10% LN hydrogel ink is the same as the blank one, while after 100% strain, it is different. The cross line of G' and G" is observed in 5% LN hydrogel ink. This indicates that the ink has changed to a liquid state at high strain, and the viscosity also drops. Rheogram of 10% LN hydrogel ink shows a significant fluctuation at a high strain, suggesting that the structure is unstable and may have broken down, leading to a transition from solid-like to liquid-like. Adding and increasing LN content promotes structural breakdown under high strain, resulting in a different appearance of the film after printing despite identical formulation, while the blank film remains more elastic even at a high strain, with the most stable structure, as shown in Table 1. Previous research used a similar formulation to our blank film with KC, XG and sucrose for 3D printing (Avallone et al., 2023). Although their results suggest that G' and G" decreased with increasing temperature, both studies showed that KC and XG gave viscoelastic rather than liquid behaviour. While sucrose enhanced thermal gel strength in a previous study, our findings revealed that LN reduced structural stability under high strain.

CONCLUSIONS

This study developed a 3D-printed multilayered hydrogel formulation containing HA and LN for hydrating and antibacterial activity. It was found that KC and XG with GR are the optimal base formulation for 3D printing. Storage at room temperature with the lid gave the best stability. The 10% LN film showed higher LN release, stronger antibacterial activity, and FT-IR of it confirmed the presence of LN, while the 5% LN film offered better tensile strength. This indicates that the formulation balances mechanical strength and antimicrobial function, which leads to anti-acne ability. Adding LN causes a structural breakdown, causing a different appearance of the film after printing. However, the focus was on the first layer of the film. Future research should investigate multilayered interactions, incorporate other active ingredients for multifunctionality in the multilayered film, and assess hydrating capacity or long-term efficacy to advance this film for cosmetic applications.

Acknowledgements

We are grateful for technical support from Liverpool John Moores University.

Conflict of interest

The authors declare no conflict of interest.

Authors contributions

CRediT: PK: Conducting experiments and writing the manuscript, SDS: writing and editing the manuscript and providing scientific discussions, TE: writing manuscript and planning experiments.

References

Avallone, P. R., Russo Spena, S., Acierno, S., Esposito, M. G., Sarrica, A., Delmonte, M., Pasquino, R. & Grizzuti, N. (2023). Thermorheological Behavior of κ-Carrageenan Hydrogels Modified with Xanthan Gum. *Fluids (Basel),* 8**,** 119.

Boriwanwattanarak, P., Ingkaninan, K., Khorana, N. & Viyoch, J. (2008). Development of curcuminoids hydrogel patch using chitosan from various sources as controlled-release matrix. *International journal of cosmetic science,* 30**,** 205-218.

Bravo, B., Correia, P., Gonçalves Junior, J. E., Sant'anna, B. & Kerob, D. (2022). Benefits of topical hyaluronic acid for skin quality and signs of skin aging: From literature review to clinical evidence. *Dermatologic therapy,* 35**,** e15903.

Chelu, M. (2024). Hydrogels with Essential Oils: Recent Advances in Designs and Applications. *Gels,* 10**,** 636.

Chen, Z., Zhao, D., Liu, B., Nian, G., Li, X., Yin, J., Qu, S. & Yang, W. (2019). 3D Printing of Multifunctional Hydrogels. *Advanced functional materials,* 29**,** 1900971.

Ehtezazi, T., Kteich, A., Abdulkarim, R., Lynch, R., Algellay, M., Mccloskey, A. P., ... & Sarker, S. D. (2023). Quantification of linalool in 3d printed fast-dissolving oral films by a high-pressure liquid chromatography method. *Journal of Natural Products Discovery,* 2(2)**,** 1-9.

Gonçalves, S., Mansinhos, I. & Romano, A. (2020). Chapter 11 - Aromatic plants: A source of compounds with antioxidant and neuroprotective effects. *In:* Martin, C. R. & Preedy, V. R. (eds.) *Oxidative Stress and Dietary Antioxidants in Neurological Diseases.* Academic Press, 155-173.

Hussain, A. I., Anwar, F., Hussain Sherazi, S. T. & Przybylski, R. (2008). Chemical composition, antioxidant and antimicrobial activities of basil (Ocimum basilicum) essential oils depends on seasonal variations. *Food chemistry,* 108**,** 986-995.

Kuo, C.-C., Qin, H., Cheng, Y., Jiang, X. & Shi, X. (2021). An integrated manufacturing strategy to fabricate delivery system using gelatin/alginate hybrid hydrogels: 3D printing and freeze-drying. *Food hydrocolloids,* 111**,** 106262.

Lee, T.-W., Kim, J.-C. & Hwang, S.-J. (2003). Hydrogel patches containing Triclosan for acne treatment. *European journal of pharmaceutics and biopharmaceutics,* 56**,** 407-412.

Li, H., Liu, M., Li, J., Zhang, X., Zhang, H., Zheng, L., Xia, N., We I, A. & Hua, S. (2024). 3D Printing of smart labels with curcumin-loaded soy protein isolate. *International journal of biological macromolecules,* 255**,** 128211.

Li, W., Yu, Y., Huang, R., Wang, X., Lai, P., Chen, K., Shang, L. & Zhao, Y. (2023). Multi‐Bioinspired Functional Conductive Hydrogel Patches for Wound Healing Management. *Advanced science,* 10**,** e2301479.

Lubart, R., Yariv, I., Fixler, D. & Lipovsky, A. (2019). Topical Hyaluronic Acid Facial Cream with New Micronized Molecule Technology Effectively Penetrates and Improves Facial Skin Quality: Results from In-vitro, Ex-vivo , and In-vivo (Open-label) Studies. *The Journal of clinical and aesthetic dermatology,* 12**,** 39-44.

Manousi, E., Chatzitaki, A.-T., Vakirlis, E., Karavasili, C. & Fatouros, D. G. (2024). Development and in vivo evaluation of 3D printed hydrogel patches for personalized cosmetic use based on skin type. *Journal of drug delivery science and technology,* 92**,** 105306.

Menezes, P. P., Serafini, M. R., Quintans-Júnior, L. J., Silva, G. F., Oliveira, J. F., Carvalho, F. M. S., Souza, J. C. C., Matos, J. R., Alves, P. B., Matos, I. L., Hădărugă, D. I. & Araújo, A. a.

S. (2014). Inclusion complex of (−)-linalool and β-cyclodextrin. *Journal of Thermal Analysis and Calorimetry,* 115**,** 2429-2437.

Pereira, I., Severino, P., Santos, A. C., Silva, A. M. & Souto, E. B. (2018). Linalool bioactive properties and potential applicability in drug delivery systems. *Colloids and surfaces, B, Biointerfaces,* 171**,** 566-578.

Phumlek, K., Itharat, A., Pongcharoen, P., Chakkavittumrong, P., Lee, H.-Y., Moon, G.-S., Han, M.-H., Panthong, S., Ketjinda, W. & Davies, N. (2022). Garcinia mangostana hydrogel patch: bactericidal activity and clinical safety for acne vulgaris treatment. *Research in pharmaceutical sciences,* 17**,** 457-467.

Shin, J., Choi, S., Kim, J. H., Cho, J. H., Jin, Y., Kim, S., Min, S., Kim, S. K., Choi, D. & Cho, S. W. (2019). Tissue Tapes–Phenolic Hyaluronic Acid Hydrogel Patches for Off‐the‐Shelf Therapy. *Advanced functional materials,* 29**,** 1903863.

Unalan, I., Schruefer, S., Schubert, D. W. & Boccaccini, A. R. (2023). 3D-Printed Multifunctional Hydrogels with Phytotherapeutic Properties: Development of Essential Oil-Incorporated ALG-XAN Hydrogels for Wound Healing Applications. *ACS Biomaterials Science & Engineering,* 9**,** 4149-4167.

Wang, J., Abbas, S. C., Li, L., Walker, C. C., Ni, Y. & Cai, Z. (2024). Cellulose Membranes: Synthesis and Applications for Water and Gas Separation and Purification. *Membranes (Basel),* 14**,** 148.

Wang, Z., Liu, L., Xiang, S., Jiang, C., Wu, W., Ruan, S., Du, Q., Chen, T., Xue, Y., Chen, H., Weng, L., Zhu, H., Shen, Q. & Liu, Q. (2020). Formulation and Characterization of a 3D-Printed Cryptotanshinone-Loaded Niosomal Hydrogel for Topical Therapy of Acne. *AAPS PharmSciTech,* 21**,** 159.